Langmuir

Article

pubs.acs.org/Langmuir

Organo-Soluble Porphyrin Mixed Monolayer-Protected Gold Nanorods with Intercalated Fullerenes

Chenming Xue,[†] Yongqian Xu,[‡] Yi Pang,[‡] Dingshan Yu,[§] Liming Dai,[§] Min Gao,[†] Augustine Urbas,[∥] and Quan Li*,[†]

[†]Liquid Crystal Institute, Kent State University, Kent, Ohio 44242, United States

[‡]Department of Chemistry and Maurice Morton Institute of Polymer Science, The University of Akron, Akron, Ohio 44325, United States

[§]Department of Chemical Engineering, Case Western Reserve University, Cleveland, Ohio 44106, United States

[∥]Materials and Manufacturing Directorate, Air Force Research Laboratory, WPAFB, Ohio 45433, United States

Supporting Information

ABSTRACT: Organo-soluble porphyrin mixed monolayer-protected gold nanorods were synthesized and characterized. The resulting gold nanorods encapsulated by both porphyrin thiol and alkyl thiol on their entire surface with strong covalent Au−S linkages were very stable in organic solvents without aggregation or decomposition and exhibited unique optical properties different from their corresponding spherical ones. Alkyl thiol acts as a stabilizer not only to fill up the potential space on gold nanorod surface between bulky porphyrin molecules but also to provide space for further insertion of C_{60} molecules forming a stable C_{60}-porphyrin-gold nanorod hybrid nanostructure.

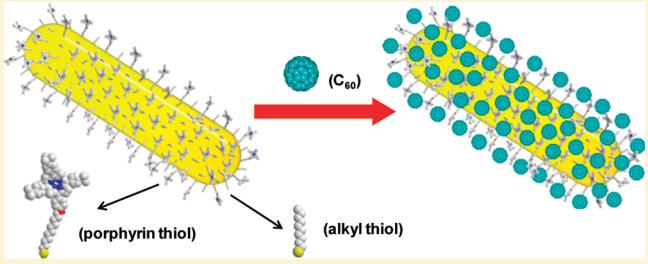

INTRODUCTION

Building metal nanoparticles protected by functional organic molecules is a rapidly growing fascinating and challenging scientific area of contemporary interest. Gold nanorods (GNRs), providing many promising applications in optics,[1] sensors,[2] biological imaging,[3] and anticancer agents[4] due to their extraordinary shape- and surface chemical environment-dependent optical properties, are among the most exciting materials today. They are quite different from the widely investigated spherical gold nanoparticles (GNPs),[5] including more distinguished physical properties[1a,6] particularly for their tunable absorption in the visible and near IR region. Besides, since anisotropic metal nanoparticles can give higher sensitivity than spherical ones in surface plasmon shift, GNRs are highly suitable for plasmon sensing with a high-value shape factor (surface curvature).[7] Also nanoparticle shape plays an important role in surface-enhanced Raman scattering enhancement (SERS). The enhancement factors on the order of 10^4−10^5 were observed for absorbed molecules on the GNRs, while no such enhancement was observed on spherical nanoparticles under similar conditions.[8]

It is well established that modifying the chemical composition of GNR surfaces provides a versatile means to tune their properties. For example, with dye molecules on GNRs, photothermal therapy and fluorescence imaging can be accomplished simultaneously.[4b] Although the coupling of dye molecules and GNRs has been implemented via ionic interactions,[9] the dynamically unstable bilayer cetyltrimethylammonium bromide (CTAB) structure on GNRs has been a problem limiting their potential applications. In these cases, thiol molecules may have an advantage because thiol monolayer-protected GNRs exhibit superior stability, accessible surface functionalization and good compatibility with organic media, in which they can disperse well. However, to date only a few thiol monolayer-protected GNRs have been reported as the seemingly trivial work of exchanging CTAB with organic thiol molecules to form thiol-monolayer-protected GNRs is challenging.[10]

For chemical modification of GNRs, one class of intriguing dye molecules are porphyrins, which have been intensively studied for a range of applications over the decades due to their excellent thermal stability, charge transport ability and high light-harvesting capability.[11,12] It was discovered that when attached to spherical GNP rather than on bulk gold surfaces, the undesirable energy transfer quenching of porphyrin's singlet excited state can be suppressed.[13] Furthermore, porphyrin and fullerene (C_{60}) are an ideal donor−acceptor pair, which allows accelerated photoinduced electron transfer and slow charge recombination, leading to the generation of a long-lived charge-separated state with a high quantum yield.[14] The porphyrin−C_{60} assemblies can be stabilized by the attractive π−π interactions.[14b] It is the first time to anchor them onto anisotropic

Received: January 6, 2012
Revised: February 28, 2012
Published: March 16, 2012

   dx.doi.org/10.1021/la300096n | *Langmuir* 2012, 28, 5956−5963

gold nanoparticles and they are expected to present advantages for solar energy conversion.

Herein we report the synthesis of GNRs that are protected by porphyrin thiol **1** and 1-decanethiol molecules via strong covalent Au−S bonds on the GNR's entire surface. The resulting mixed porphyrin/thiol monolayer-protected gold nanorods (**P−C_{10}-GNR**) were very stable in organic solvents without aggregation or decomposition, and exhibited particular optical properties, in sharp contrast to the corresponding spherical GNPs, as well as, the porphyrin thiol **1**. The alkyl thiol $C_{10}H_{21}SH$ acts as a stabilizer not only to fill up the potential space on GNR surface between bulky porphyrin molecules, but also to provide space for further insertion of C_{60} molecules. Owing to the presence of $C_{10}H_{21}SH$ molecules, the shorter alkyl chains create void space between bulky porphyrin groups for C_{60} molecules, resulting in an electron donor−acceptor structure on the GNR surface. Together with **P−C_{10}-GNR**, single porphyrin monolayer-protected gold nanorods (**P-GNR**), $C_{10}H_{21}SH$ monolayer-protected gold nanorods (**C_{10}-GNR**), and porphyrin monolayer-protected spherical gold nanoparticles (**P-GNP**) were also synthesized for comparison study (see the Supporting Information). Compared with the straightforward synthesis of spherical **P-GNP**s in one step,[15] the preparation of thiol monolayer-protected GNRs is more complicated.

EXPERIMENTAL SECTION

Materials and Measurements. All chemicals and solvents were purchased from commercial supplies and used without further purification. $HAuCl_4$ is a 30 wt % in diluted HCl solution. ^1H NMR spectra were recorded on a Bruker 400 MHz NMR spectrometer, with deuterated chloroform ($CDCl_3$) as solvent at 25 °C. The chemical shifts were reported using 7.26 ppm of $CHCl_3$ residue as the internal standard. ^{13}C NMR spectra were recorded on a Varian 200 MHz NMR spectrometer, with deuterated chloroform ($CDCl_3$) as solvent. The chemical shifts were reported using 77.16 ppm of $CHCl_3$ residue as the internal standard. The NMR graphs and data were collected by using Spinworks 3 software. Fourier transfer infrared spectra (FTIR) were recorded on a Nicolet Magna-IR spectrometer 550 spectrometer at the resolution of 4 cm^{-1}. High resolution mass spectrometry (HRMS) was performed by Mass Spectrometry & Proteomics Facility of The Ohio State University. Elementary analysis was performed in Robertson Microlit Laboratories. UV−visible spectra were collected on a PerkinElmer Lambda 25 UV−vis spectrometer at the resolution of 1 nm. Fluorescence spectra were recorded on a FluoroMax-4 spectrafluorometer of Horiba scientific. The Raman spectra were obtained with a RENISHAW inVia Raman microscope instrument using a diode laser with excitation wavelength of 785 nm. Samples for Raman spectra were casted on glass slides and left to dry before measurements. Each spectrum is obtained in 10 s collection time with five accumulations. For transmission electron microscopy (TEM) observation, solution samples were first dispersed on TEM Cu grids precoated with thin carbon film (Cu-400 CN) purchased from Pacific Grid Tech. After completely dried, they were studied using a FEI Tecnai TF20 FEG TEM equipped with a EDAX energy-dispersive X-ray spectrometer (EDX) for elemental analysis.

Preparation of Porphyrin Thiol 1. The route of preparing porphyrin thiol **1** was shown in Figure 1. The porphyrin thiol **1** was synthesized starting from unsymmetrical porphyrin derivative **2**, which was reacted with 11-bromo-1-undecanol to give bromo compound **3**. Then the active bromide **3** was reacted with potassium thiol acetate to give the intermediate compound **4**. Finally intermediate **4** was deprotected in the presence of tetrabutylammonium cyanide (TBACN) to afford the product porphyrin thiol **1**. The structure of intermediate **2**−**4** was identified by ^1H NMR, ^{13}C NMR, Ft-IR, elemental analysis and HRMS. For **1**, because it was not able to be purified through column, the reaction product of **1** was characterized by ^1H NMR and HRMS, from which the yield and rightness of compound **1** can be verified (Figure S1). The details were listed in the Supporting Information.

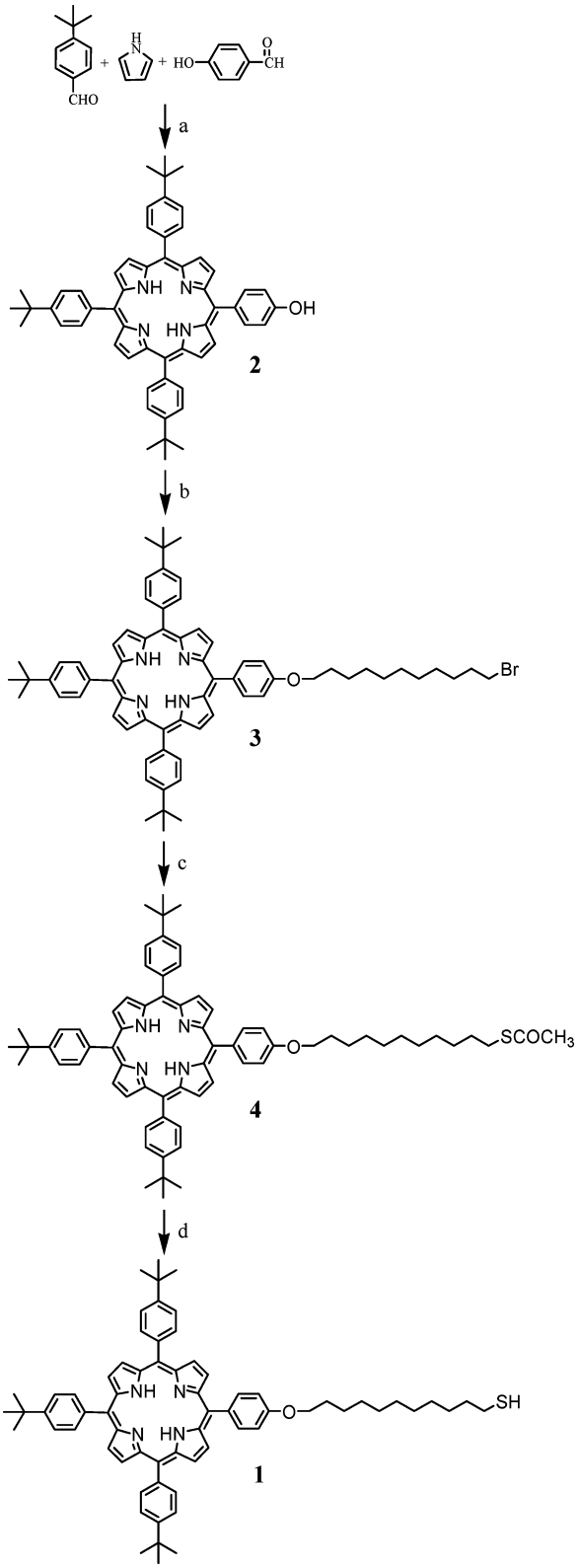

Figure 1. Synthesis of porphyrin thiol **1**. Conditions: (a) propionic acid, reflux; (b) 11-bromo-1-undecanol, DIAD, PPh_3, stir at RT; (c) CH_3COSK, acetone/$CHCl_3$ (1:1), RT, 24 h; (d) tetrabutylammonium cyanide, $CHCl_3$/MeOH (2:1), 50 °C, 24 h.

Preparation of CTAB-Coated Gold Nanorods (CTAB-GNRs). The CTAB-coated GNRs were freshly prepared by the seed-mediated

dx.doi.org/10.1021/la300096n | Langmuir 2012, 28, 5956−5963

growth method.[1a] For seed preparation, specifically, 0.5 mL of an aqueous 0.01 M solution of $HAuCl_4$ was added to CTAB solution (15 m L, 0.1 M) in a vial. A bright brown-yellow color appeared. Then, 1.20 mL of 0.01 M ice-cold aqueous $NaBH_4$ solution was added all at once, followed by rapid inversion mixing for 2 min. The solution developed a pale brown-yellow color. Then, the vial was kept in a water bath maintained at 25 °C for future use. For nanorods growth, 9.5 mL of 0.1 M CTAB solution in water was added to a tube, and 0.40 mL of 0.01 M $HAuCl_4$ and 0.06 mL of 0.01 M $AgNO_3$ aqueous solutions were added in this order and mixed by inversion. Then, 0.06 mL of 0.1 M of ascorbic acid solution was added, and the resulting mixture at this stage became colorless. The seed solution (0.02 mL) was added to the above mixture tube, and the tube was slowly mixed for 10 s and left to sit in the water bath at 25−30 °C for 3 h. The final solution turned purple within minutes after the tube was left undisturbed.

Porphyrin Thiol Monolayer Protected Gold Nanorods (P-GNRs). The solution of CTAB-GNRs was centrifuged at 7500 rpm per 20 min several times to remove the excessive CTAB and other solution components and redispersed in 1.5 mL of water. Then, this aqueous solution of GNRs was added dropwise to a solution of the thiol **1** (50 mg) in 40 mL THF with stirring under the protection of nitrogen. The color of the reaction mixture is purple. The reaction mixture was continued to stir at room temperature for 3 days and centrifuged. To improve the GNRs with thiol molecules over the surface, the precipitates were dispersed in $CHCl_3$ and sonicated, 10 mg thiol **1** were added into the solutions. The solution was stirred for another 24 h and centrifuged. This procedure was repeated another three times. The as-prepared GNRs were centrifuged and washed with $CHCl_3$ several times until there was no UV or ^1H NMR signal in the top layer solution, which means there were no free thiols in the system. The resulting GNRs were named as **P-GNRs**.

Decanethiol Monolayer Protected Gold Nanorods (C_{10}-GNRs). The synthesis method was the same as above. The thiol molecule $C_{10}H_{21}SH$ (30 mg) was used for the first exchange, and 10 mg was used for each of the next steps for complete surface protection.

Porphyrin Thiol and Decanethiol Monolayer Protected Gold Nanorods (P-C_{10}-GNRs). The synthesis method was the same as above. The porphyrin thiol **1** (56 mg, 0.057 mmol) was mixed with CTAB-GNR first, and then $C_{10}H_{21}SH$ (10 mg, 0.057 mmol) was added slowly. A total of 5 mg of **1** and 10 mg of $C_{10}H_{21}SH$ were used for each of the next steps for complete surface protection.

Synthesis of Porphyrin-Thiol Monolayer Protected Spherical Gold Nanoparticles (P-GNPs). The route is based on that in ref 15a with some modifications. An aqueous solution of hydrogen tetrachloroaurate (3 mL, 30 mmol/L) was mixed with a solution of tetraoctylammonium bromide in toluene (8 mL, 50 mmol/L). The two-phase mixture was vigorously stirred until all of the tetrachloroaurate was transferred into the organic layer. The water layer was removed, and 50 mg of **1** was then added to the organic phase. A freshly prepared aqueous solution of sodium borohydride (2.5 mL, 0.4 mol/L) was slowly added with vigorous stirring. After further stirring for 3 h, the organic phase was separated, evaporated to 1 mL in a rotary evaporator, and mixed with 40 mL of ethanol. The mixture was kept for 4 h at −18 °C. The crude product was filtered and washed with ethanol. The solid was dissolved in $CHCl_3$ and centrifuged at 14 000 rpm for 12 min. After centrifugation, the top layer was removed and the solid was sonicated after adding $CHCl_3$. This wash step was carried several times until the top layer did not have UV or vis absorption signal for free porphyrin molecules. Afterward, the **P-GNP** in $CHCl_3$ was obtained.

Preparation of C_{60}-P-C_{10}-GNR. For inserting fullerenes (C_{60}) into the **P-C_{10}-GNR** or **P-GNR**, about 0.4 mg corresponding NRs was dissolved in 2 mL of 1:1 (v/v) toluene/CH_3CN. Saturated C_{60} toluene solution (3 mg/mL) was added by drops. The mixture was stirred at room temperature. The prepared **C_{60}-P-C_{10}-GNR** and **C_{60}-P-GNR** solutions were centrifuged. Then the top layer was removed, 2 mL of $CHCl_3$ was added and the mixture was sonicated. After washed with $CHCl_3$ several times until there was no UV absorption in the top layer, which means there was no free C_{60} in the solvent, $CHCl_3$ (2 mL) was added and the solid was sonicated and dispersed well.

I_2 Induced Decomposition of P-C_{10}-GNR. In a typical procedure, ca. 2 mg of **P-C_{10}-GNR** was dissolved in $CDCl_3$ and its ^1H NMR spectrum was collected. Then, 1 mg of iodine was added to this solution and followed by stirring at room temperature for 3 h. The decomposition process could be monitored by a change in solution color from purple to dark red-purple. After removal of bulky gold by centrifuging, the clear top layer solution was collected and dried. After it was dissolved in $CDCl_3$, the ^1H NMR spectrum was collected and it was compared with that from before decomposition. For fluorescence experiment, since the excess I_2 made the solution pink-red color, the aqueous $(NH_4)_2SO_3$ solution (0.5 M) was added to the above organic solution and it was shaken vigorously. Afterward, the aqueous layer was removed. **P-GNP** and **P-GNR** were treated the same way for releasing porphyrin thiols.

RESULTS AND DISCUSSION

Raman spectra (Figure 2) exhibited a characteristic Au−Br band at 180 cm^{-1} for CTAB-coated gold nanorods (**CTAB-GNR**)

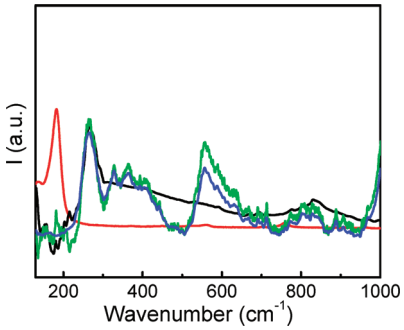

Figure 2. Raman spectra of the **CTAB-GNR** (red), **P-C_{10}-GNR** (blue), **P-GNR** (green), and **C_{10}-GNR** (black).

and a characteristic Au−S band at 260 cm^{-1} accompanied with the disappearance of the Au−Br band for **P-C_{10}-GNR**, **P-GNR**, and **C_{10}-GNR**,[8,16] which indicated the successful removal of bromide and covalent bonding of the thiol molecule to the gold surface. In order to further confirm that the thiol molecules indeed replaced CTAB molecules on the GNR surface, energy-dispersive X-ray spectroscopy (EDX) was performed (Figure S2). It can be seen that the S peak appeared for **P-C_{10}-GNR** with the disappearance of the Br peak. Besides, ^1H NMR (Figure 3)

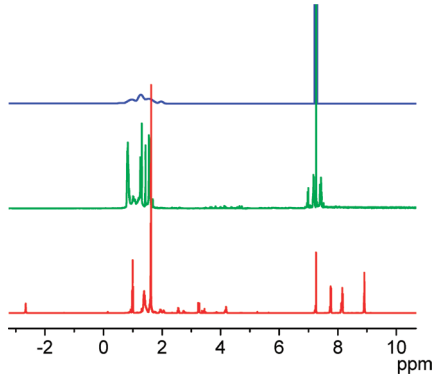

Figure 3. ^1H NMR spectra of **P-C_{10}-GNR** (blue), mixture residue after I_2 induced decomposition (green) and **1** after reducing reaction (red).

dx.doi.org/10.1021/la300096n | Langmuir 2012, 28, 5956−5963

measurements show that the peaks became broadened and weaker than those of the free porphyrin **1** molecules, similar to the results of other GNRs.[10c] The reasons for this broadening effect have been raised: (a) the tight packing of protons close to the Au core causes rapid spin−spin relaxation from dipolar interactions; (b) there are different chemical shifts for surface heterogeneities (different nanocrystalline faces: vertexes, edges, and terraces), and the chemical shifts vary with core size and defect; and (c) slow rotational diffusion of the clusters (analogous to effects seen for large proteins) depending on nanoparticle size.[10e] Although the signals of porphyrin thiols could not be observed on GNRs, they reappeared after being detached from GNRs. After degradation by adding I_2, the composition of thiol molecules on **P-C$_{10}$-GNR** can be calculated (Figure 3). The following is the way to calculate the ratio of porphyrin **1** to $C_{10}H_{21}SH$. In the green cruve, the ratio of integration areas of the aromatic part to the alkyl part is 1:3. Since for porphyrin thiol **1** the porphyrin core part has 24 H (aromatic) and alkyl part has 50 H, we can calculate the integration of protons from $C_{10}H_{21}SH$ as $3 - 1/24 \times 50 = 0.92$ from the green curve (as the integration of porphyrin aromatic H = 1). Therefore, the ratio of **1** to $C_{10}H_{21}SH$ is (1/24):(0.92/22), approximately 1:1. Thus, it is a 1:1 ratio of thiol **1** to $C_{10}H_{21}SH$ on **P-C$_{10}$-GNR**.

UV−vis absorption spectra of **CTAB-GNR**, **P−C$_{10}$-GNR** and spherical **P-GNP** are shown in Figure 4. Stable organo-

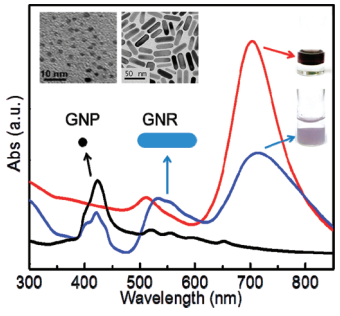

Figure 4. UV−vis spectra of **CTAB-GNR** in H_2O (red), **P-C$_{10}$-GNR** (blue), and spherical **P-GNP** (black) in $CHCl_3$. The insets show photographs of the solutions of corresponding **CTAB-GNR** (right-top) and **P-C$_{10}$-GNR** (right-bottom) in the two phases (top layer, water; bottom layer, $CHCl_3$) and TEM images of **P-GNP** (left) and **P-C$_{10}$-GNR** (right).

soluble **P−C$_{10}$-GNR** and spherical **P-GNP** were observed by TEM, showing they were well dispersed with no aggregation (insets in Figure 4). **P-C$_{10}$-GNR** displayed an average size of 44 nm ×13 nm and an approximate aspect ratio of 3.4 based on calculating 500 nanorods. Spherical **P-GNP** had an average diameter of 2.3 nm. The existence of typical porphyrin peak at 421 nm indicated the bonding of porphyrin thiol **1** on GNR. After a successful exchange with thiols, the nanoparticles were moved from aqueous media to organic solvent. In contrast to UV−vis absorption spectrum of the spherical **P-GNP**, two characteristic plasmon peaks were observed for both **CTAB-GNR** and **P-C$_{10}$-GNR**. The strong longitudinal peak in the near-infrared region (710 and 714 nm, respectively) corresponds to the electron oscillation along the long axis, and a weak transverse peak in the visible region (513 and 533 nm, respectively) is due to electron oscillation along the short axis. The red-shift of the longitudinal and transverse peaks for **P-C$_{10}$-GNR** results from the change of dielectric constant around GNR due to attachment of the porphyrin **1**. Without porphyrin **1**, **C$_{10}$-GNR** did not show such red shift for either of these two peaks (Figure 5). Notably, the transverse peak shows

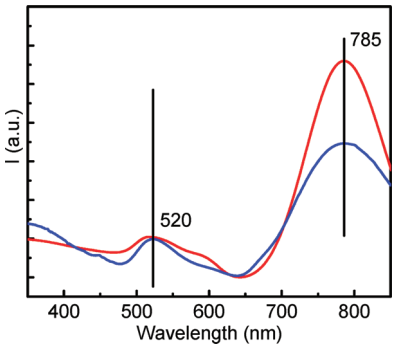

Figure 5. The UV−vis spectra of **CTAB-GNR** in H_2O (red) and **C$_{10}$-GNR** in $CHCl_3$ (blue).

a large red-shift (about 20 nm), which could be ascribed to the side-by-side arrangement of nanorods in solution.[17] However, since there was neither accompanying blue-shift of the longitudinal band, nor any prominent side-by-side assembly of GNRs observed by TEM (inset of Figure 4 and Figure S3), the peak shift can only be attributed to the influence of porphyrin **1**. Additionally, UV−vis absorption spectra and TEM images of **P-GNR** (with only porphyrin **1** on GNR surface) were shown in Figure 6. The appearance of characteristic

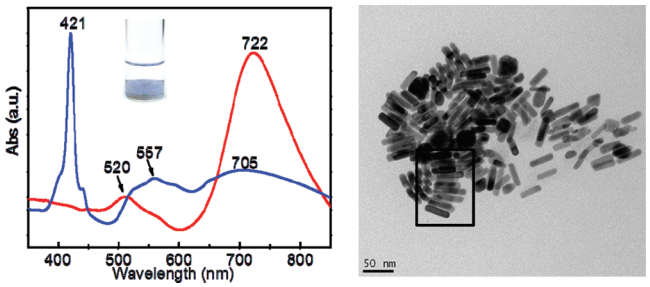

Figure 6. Left: UV−vis of **CTAB-GNR** (red) and **P-GNR** (blue) (inset: the picture of **P-GNR** in $CHCl_3$ showing bluish color, top layer is water). Right: TEM image of **P-GNR**, indicating the existence of side-by-side assembly.

porphyrin peak (421 nm) indicated the binding of **1** onto these GNRs. However, its $CHCl_3$ solution displayed a bluish color, and the UV−vis absorption spectra showed that the two SPR peaks broadened. Also there was significant red-shift for transverse SPR (from 520 to 557 nm) and blue shift for longitudinal SPR (from 722 to 705 nm). This implies the side-by-side assembling of GNRs, which was observed by TEM. The attractive $\pi-\pi$ interaction of porphyrin chromophores could be the interpretation for the assembly of **P-GNR**.

Fluorescence spectra (Figure 7a,b) also revealed the distinctively different patterns for all of these prepared nanoparticles. After detaching from gold nanoparticles, free porphyrin thiols in $CHCl_3$ showed characteristic emission peaks at 656 and 721 nm. When being linked onto gold nanoparticles including GNPs and GNRs, the intensity significantly quenched, by almost 99%. However, for **P-GNP** the peak shape was almost the same as free porphyrins. For **P-GNR** and **P-C$_{10}$-GNR**, the peak intensity and shape were similar. Different from free porphyrins and **P-GNP**, the peak at 712 nm was relatively

dx.doi.org/10.1021/la300096n | *Langmuir* 2012, 28, 5956−5963

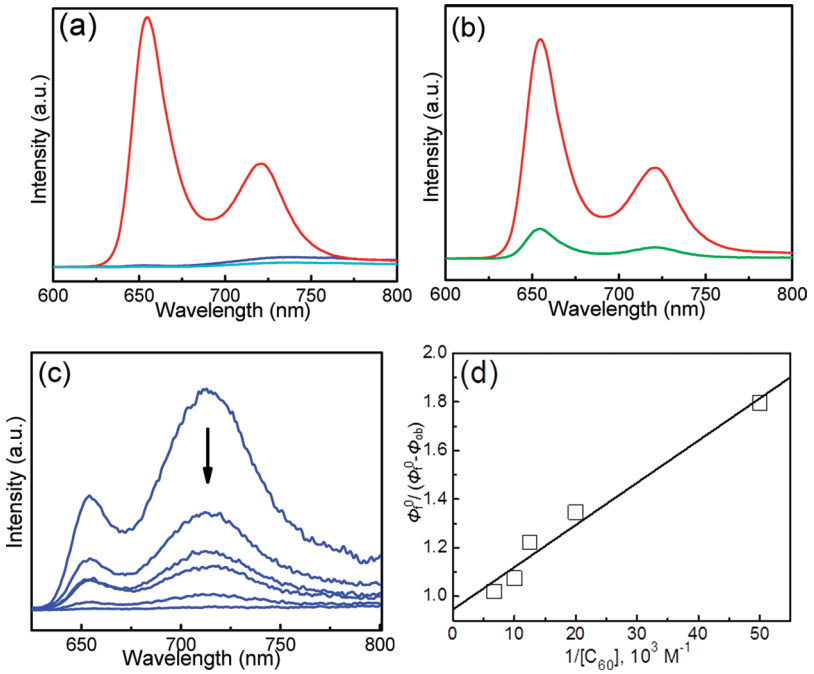

Figure 7. (a) Fluorescence spectra of free porphyrins detached from **P-C$_{10}$-GNR** (red) (diluted for ten times), **P-C$_{10}$-GNR** (blue), and **P-GNR** (cyan) in $CHCl_3$ with excitation wavelength at 420 nm. For **P-GNR** the intensity of free porphyrin thiols was normalized to be the same as from **P-C$_{10}$-GNR**. (b) Fluorescence spectra of free porphyrins detached from **P-GNP** (red) (diluted for ten times) and **P-GNP** (green) in $CHCl_3$ with excitation wavelength at 420 nm. (c) The quench of **P-C$_{10}$-GNR** in 1:1 (v/v) toluene/CH_3CN (0.2 mg in 2 mL mixture) upon the addition of C_{60} (C_{60} concentrations from top to bottom: 0, 0.02, 0.05, 0.08, 0.1, and 0.15 mM). (d) Dependence of $\Phi_f^0/(\Phi_f^0 - \Phi_f(ob))$ on the reciprocal concentration of C_{60} in acetonitrile/toluene, 1/1.

much stronger than the 656 nm peak. This indicated that there exist the interaction between the porphyrin and gold nanoparticles, and the photoelectronic properties of porphyrin chromophores are significantly altered when closely bound to GNRs.

The formation of C_{60}-GNR conjugations was verified by further fluorescence quenching in toluene/CH_3CN mixture for **P-C$_{10}$-GNR** in Figure 7c, even though the fluorescence of porphyrin chromophores has been significantly quenched by GNRs. The association constant for the formation of **P-C$_{10}$-GNR** and C_{60} complex has been calculated based on the fluorescence quenching in Figure 7c,d. After simplified treatment,[18] the formula is

$$\frac{1}{\Phi_f^0 - \Phi_{f(ob)}^0} = \frac{1}{\Phi_f^0 - \Phi_f'} + \frac{1}{K(\Phi_f^0 - \Phi_f')[C_{60}]}$$

Φ_f^0 is the fluorescence quantum yield of uncomplexed **P-C$_{10}$-GNR**, Φ_f' is the complexed one, $\Phi_{f(ob)}^0$ is the observed yield, and K is the association constant. Φ_f' is considered to be 0 when the complex is completely formed. By using this equation, a linear dependence of $1/(\Phi_f^0 - \Phi_{f(ob)}^0)$ on the concentration of C_{60} can be obtained. After linear fit, the constant K is calculated from the slope. The K value is 58 600 M^{-1}.

After removing free C_{60} in solution by repeated centrifugation and ultrasonication, the successful intercalation of C_{60} on **P-C$_{10}$-GNR** was further examined by monitoring their characteristic UV–vis absorption spectra peak (see Figure 8 top), whereas spectroscopic evidence of C_{60} could not be found in **P-GNR** when insertion of C_{60} was performed under the same experimental conditions. TEM provides direct evidence for the C_{60} intercalation. As shown in Figure 8 bottom, a sharp boundary can be observed between the edge of **P-C$_{10}$-NR** and

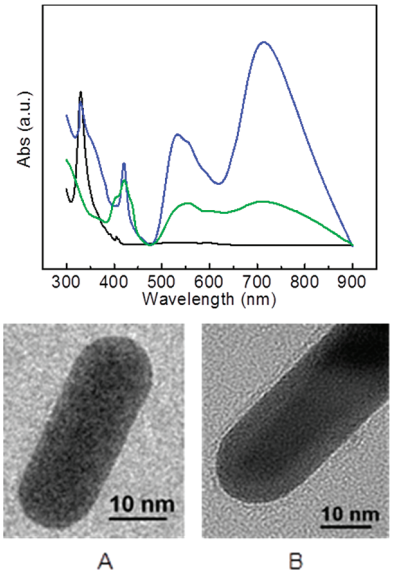

Figure 8. (Top) UV–vis spectra of **P-C$_{10}$-GNR** (blue) and **P-GNR** (green) after washing away free C_{60} in solution. Solution of C_{60} (black) has also been presented for referring. (Bottom) TEM images of **P-C$_{10}$-GNR** (A) and **C$_{60}$-P-C$_{10}$-GNR** conjugate. Note: The diffusion layer on the edge of **P-C10-GNR** (B) indicates the existence of C_{60} molecules.

the supporting carbon film (A), whereas a thin layer can be identified on the nanorod surface (B) after the addition of C_{60} followed by removing free C_{60} molecules in solution, supporting the conjecture of the sandwiched C_{60} molecules in the hybrid GNRs. The combination of $C_{10}H_{21}SH$ molecules and porphyrin molecules enabled the insertion of C_{60}, creating

dx.doi.org/10.1021/la300096n | *Langmuir* 2012, 28, 5956–5963

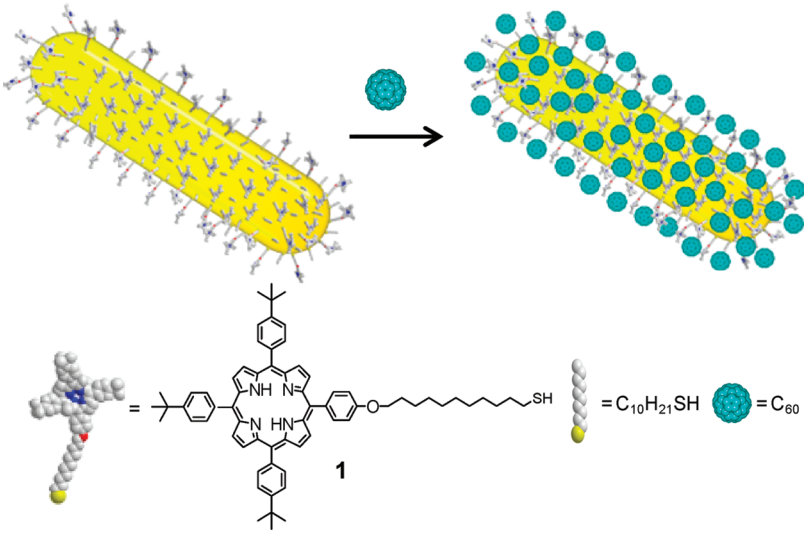

Figure 9. Schematic representation of **P-C_{10}-GNR** intercalated with C_{60} and chemical structure of our synthesized porphyrin thiol **1** and commercially available 1-decanethiol.

the electron donor−acceptor alternative structure on the GNR surface. A schemetic illustration of this hybrid structure has been presented in Figure 9.

Structural details of thiol molecules on **P-C_{10}-GNR** and **P-GNR** were described in Figure 10, which showed the feasibility

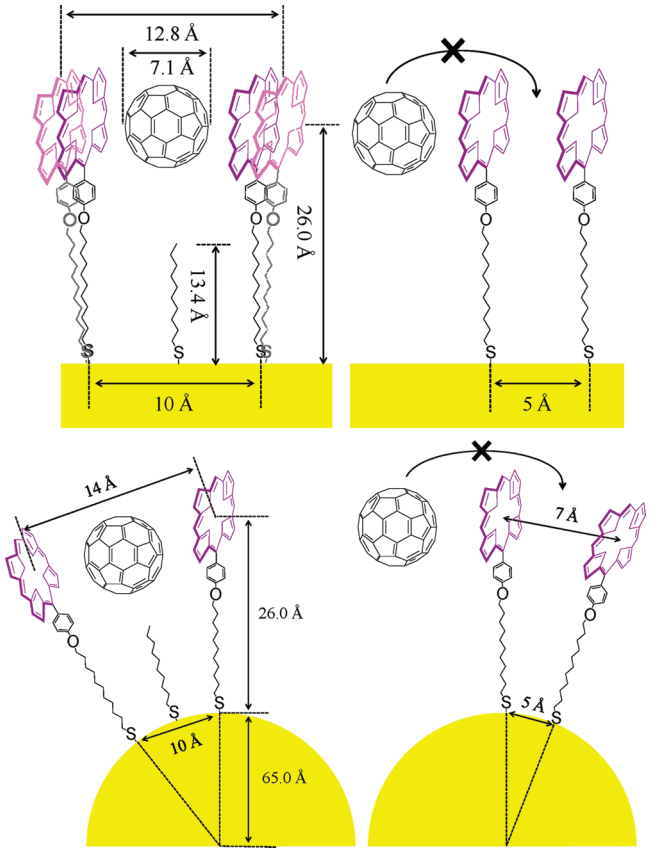

Figure 10. Schematic interpretation of feasible intercalation of C_{60} into **P-C_{10}-GNR** instead of **P-GNR**. The top pictures are from the side view of GNR, and the bottom pictures are from the section view. The *t*-butylphenyl groups at porphyrin core are omitted for clarity.

of intercalating C_{60} between porphyrin molecules on **P-C_{10}-GNR** but not on **P-GNR**. Due to the curvature of the small spherical GNPs (ca. 2 nm), there was a suitable void space for C_{60} to insert between two porphyrin groups.[18] In the case of **P-GNR**, the surface curvature is insufficient to provide such a void space. On GNR surface, the average distance between two gold atoms to which thiol molecules are attached is about 5 Å.[19] For **P-C_{10}-GNR**, between two **1** molecules it is about 10 Å with one $C_{10}H_{21}SH$ molecule standing in the middle. From center of porphyrin **1** to the surface of GNR, it is about 26 Å and the longest chain length of $C_{10}H_{21}SH$ is 13.4 Å away from the GNR surface. It can be calculated as 12.6 Å from the center of porphyrin ring to $C_{10}H_{21}SH$ chain, which is much larger than 7.1 Å, the diameter of a C_{60} molecule.[18] The closest distance between a carbon of C_{60} and the center of the porphyrin ring has been reported as 2.856 Å.[20] The smallest center-to-center distance of two porphyrin chromophores which can sandwich a C_{60} molecule is about 12.8 Å by adding the diameter of C_{60} to twice the closest distance between C_{60} and a porphyrin ring. With the flexible *n*-alkyl part of **1** which has 11 CH_2 units, the two **1** molecules on **P-C_{10}-GNR** can tilt slightly to accommodate a C_{60} molecule, as shown in the top left picture. On the other hand, for **P-GNR**, since there is no short chain on the surface to provide the void space, C_{60} molecules could not be sandwiched by porphyrin molecules. The section view of GNR has also been presented to illustrate the feasible intercalation of C_{60} on **P-C_{10}-GNR** and infeasible intercalation on **P-GNR**. The lengths of porphyrin molecule **1** and $C_{10}H_{21}SH$ were calculated in Chem 3D of ChemDraw.

CONCLUSION

In conclusion, porphyrin mixed monolayer-protected GNRs were for the first time synthesized and characterized. The resulting porphyrin GNRs showed unique optical properties in sharp contrast to their corresponding spherical GNPs. With the short alkyl thiol molecules, **P-C_{10}-GNR** enabled the insertion of C_{60}, creating the electron donor−acceptor alternative structure on the GNR surface. Through this hybrid nanomaterial, it opens a new avenue for research in investigating the effects of functional organic molecules on the plasmonic properties of

dx.doi.org/10.1021/la300096n | *Langmuir* 2012, 28, 5956−5963

anisotropic gold nanoparticles. This hybrid structure holds promise for energy conversion in hybrid photovoltaic devices by providing increasing donor−acceptor interface for the porphyrin−C_{60} system with the huge contact area. In addition, for future study, when the alkyl of porphyrin thiols and *n*-alkyl chains are shortened which pulls the porphyrin groups and C_{60} molecules closer to GNR surface (<1 nm), the nanorod structure could be used as a direct path for charge transport, a key requirement for efficient photovoltaic devices. This combination of an organic electron donor−acceptor system and inorganic NRs could be used to enhance the capability of photovoltaic devices and improve their performances.

■ ASSOCIATED CONTENT

Supporting Information

Details of thiol synthesis, the interpretation of successful synthesis of **1**, Raman spectra, EDX spectra, and TEM images of **P-C_{10}-GNR** with larger size scale bars. This material is available free of charge via the Internet at http://pubs.acs.org.

■ AUTHOR INFORMATION

Corresponding Author

*E-mail: qli1@kent.edu.

Notes

The authors declare no competing financial interest.

■ ACKNOWLEDGMENTS

This work was supported by the Air Force Office of Scientific Research (AFOSR FA9550-09-1-0254). Discussions with X. Ma and Y. Li are acknowledged. The TEM data were obtained at the (cryo) TEM facility at the Liquid Crystal Institute, Kent State University, supported by the Ohio Research Scholars Program Research Cluster on Surfaces in Advanced Materials.

■ REFERENCES

(1) (a) Murphy, C. J.; San, T. K.; Gole, A. M.; Orendorff, C. J.; Gao, J. X.; Gou, L.; Hunyadi, S. E.; Li, T. Anisotropic Metal Nanoparticles: Synthesis, Assembly, and Optical Applications. *J. Phys. Chem. B* **2005**, *109*, 13857−13870. (b) Burda, C.; Chen, X. B.; Narayanan, R.; El-Sayed, M. A. Chemistry and Properties of Nanocrystals of Different Shapes. *Chem. Rev.* **2005**, *105*, 1025−1102. (c) Zhou, J.; Dong, J.; Wang, B.; Koschny, T.; Kafesaki, M.; Soukoulis, C. M. Negative Refractive Index due to Chirality. *Phys. Rev. B* **2009**, *79*, 121104.

(2) (a) Li, C. Z.; Male, K. B.; Hrapovic, S.; Luong, J. H. T. Fluorescence Properties of Gold Nanorods and Their Application for DNA Biosensing. *Chem. Commun.* **2005**, 3924−3926. (b) Yu, C. X.; Irudayaraj, J. Multiplex Biosensor Using Gold Nanorods. *Anal. Chem.* **2007**, *79*, 572−579. (c) Sudeep, P. K.; Joseph, S. T. S.; Thomas, K. G. Selective Detection of Cysteine and Glutathione Using Gold Nanorods. *J. Am. Chem. Soc.* **2005**, *127*, 6516−6517.

(3) (a) Huang, X. H.; El-Sayed, I. H.; Qian, W.; El-Sayed, M. A. Cancer Cell Imaging and Photothermal Therapy in The Near-Infrared Region by Using Gold Nanorods. *J. Am. Chem. Soc.* **2006**, *128*, 2115−2120. (b) Pissuwan, D.; Valenzuela, S. M.; Miller, C. M.; Cortie, M. B. A Golden Bullet? Selective Targeting of Toxoplasma Gondii Tachyzoites Using Anti Body-Functionalized Gold Nanorods. *Nano Lett.* **2007**, *7*, 3808−3812. (c) Ding, H.; Yong, K. T.; Roy, I.; Pudavar, H. E.; Law, W. C.; Bergey, E. J.; Prasad, P. N. Gold Nanorods Coated with Multilayer Polyelectrolyte as Contrast Agents for Multimodal Imaging. *J. Phys. Chem. C* **2007**, *111*, 12552−12557.

(4) (a) Chen, C. C.; Lin, Y. P.; Wang, C. W.; Tzeng, H. C.; Wu, C. H.; Chen, Y. C.; Chen, C. P.; Chen, L. C.; Wu, Y. C. DNA-Gold Nanorod Conjugates for Remote Control of Localized Gene Expression by Near Infrared Irradiation. *J. Am. Chem. Soc.* **2006**, *128*, 3709−3715. (b) Tong, L.; Zhao, Y.; Huff, T. B.; Hansen, M. N.; Wei, A.; Cheng, J. X. Gold Nanorods Mediate Tumor Cell Death by Compromising Membrane Integrity. *Adv. Mater.* **2007**, *19*, 3136−3141. (c) Norman, R. S.; Stone, J. W.; Gole, A.; Murphy, C. J.; Sabo-Attwood, T. L. Targeted Photothermal Lysis of The Pathogenic Bacteria, Pseudomonas Aeruginosa, with Gold Nanorods. *Nano Lett.* **2008**, *8*, 302−306.

(5) Daniel, M. C.; Astruc, D. Gold Nanoparticles: Assembly, Supramolecular Chemistry, Quantum-Size-Related Properties, and Applications toward Biology, Catalysis, and Nanotechnology. *Chem. Rev.* **2004**, *104*, 293−346.

(6) Link, S; El-Sayed, M. A. Spectral Properties and Relaxation Dynamics of Surface Plasmon Electronic Oscillations in Gold and Silver Nanodots and Nanorods. *J. Phys. Chem. B* **1999**, *103*, 8410−8426.

(7) Yu, C.; Irudayaraj, J. Quantitative Evaluation of Sensitivity and Selectivity of Multiplex NanoSPR Biosensor Assays. *Biophys. J.* **2007**, *93*, 3684−3692.

(8) Nikoobakht, B.; Wang, J. P.; El-Sayed, M. A. Surface-Enhanced Raman Scattering of Molecules Adsorbed on Gold Nanorods: Off-Surface Plasmon Resonance Condition. *Chem. Phys. Lett.* **2002**, *366*, 17−23.

(9) Ni, W. H.; Yang, Z.; Chen, H. J.; Li, L.; Wang, J. F. Coupling Between Molecular and Plasmonic Resonances in Freestanding Dye-Gold Nanorod Hybrid Nanostructures. *J. Am. Chem. Soc.* **2008**, *130*, 6692−6693.

(10) (a) Khanal, B. P.; Zubarev, E. R. Rings of Nanorods. *Angew. Chem., Int. Ed.* **2007**, *46*, 2195−2198. (b) Dai, Q.; Coutts, J.; Zou, J. H.; Huo, Q. Surface Modification of Gold Nanorods through A Place Exchange Reaction inside An Ionic Exchange Resin. *Chem. Commun.* **2008**, 2858−2860. (c) Li, Y. N.; Yu, D. S.; Dai, L. M.; Urbas, A.; Li, Q. Organo-Soluble Chiral Thiol-Monolayer-Protected Gold Nanorods. *Langmuir* **2011**, *27*, 98−103. (d) El Khoury, J. M.; Zhou, X.; Qu, L. T.; Dai, L. M.; Urbas, A.; Li, Q. Organo-Soluble Photoresponsive Azo Thiol Monolayer-Protected Gold Nanorods. *Chem. Commun.* **2009**, 2109−2111. (e) Donkers, R. L.; Lee, D.; Murray, R. W. Synthesis and Isolation of The Molecule-Like Cluster $Au_{38}(PhCH_2CH_2S)_{24}$. *Langmuir* **2004**, *20*, 1945−1952.

(11) Kadish, K. M., Smith, K. M., Guilard, R., Eds.; *The Porphyrin Handbook*; Academic Press: San Diego, 2000.

(12) Sun, Q.; Dai, L.; Zhou, X.; Li, L.; Li, Q. Bilayer- and Bulk-Heterojunction Solar Cells Using Liquid Crystalline Porphyrins as Donors by Solution Processing. *Appl. Phys. Lett.* **2007**, *91*, 253505.

(13) (a) Imahori, H.; Arimura, M.; Hanada, T.; Nishimura, Y.; Yamazaki, I.; Sakata, Y.; Fukuzumi, S. Photoactive Three-Dimensional Monolayers: Porphyrin-Alkanethiolate-Stabilized Gold Clusters. *J. Am. Chem. Soc.* **2001**, *123*, 335−336. (b) Imahori, H.; Kashiwagi, Y.; Endo, Y.; Hanada, T.; Nishimura, Y.; Yamazaki, I.; Araki, Y.; Ito, O.; Fukuzumi, S. Structure and Photophysical Properties of Porphyrin-Modified Metal Nanoclusters with Different Chain Lengths. *Langmuir* **2004**, *20*, 73−81.

(14) (a) Zhou, X.; Kang, S. W.; Kumar, S.; Kulkarni, R. R.; Cheng, S. Z. D.; Li, Q. Self-Assembly of Porphyrin and Fullerene Supramolecular Complex into Highly Ordered Nanostructure by Simple Thermal Annealing. *Chem. Mater.* **2008**, *20*, 3551−3553. (b) Sun, D.; Tham, F. S.; Reed, C. A.; Chaker, L.; Boyd, P. D. W. Supramolecular Fullerene-Porphyrin Chemistry. Fullerene Complexation by Metalated "Jaws Porphyrin" Hosts. *J. Am. Chem. Soc.* **2002**, *124*, 6604−6612 and references there in.

(15) (a) Brust, M.; Walker, M.; Bethell, D.; Schiffrin, D. J.; Whyman, R. Synthesis of Thiol-Derivatized Gold Nanoparticles in A 2-Phase Liquid-Liquid System. *J. Chem. Soc. Chem. Commun.* **1994**, 801−802. (b) Zhou, X.; El Khoury, J. M.; Qu, L.; Dai, L.; Li, Q. A Facile Synthesis of Aliphatic Thiol Surfactant with Tunable Length as A Stabilizer of Gold Nanoparticles in Organic Solvents. *J. Colloid Interface Sci.* **2007**, *308*, 381−384.

(16) Huang, X. H.; Neretina, S.; El-Sayed, M. A. Gold Nanorods: From Synthesis and Properties to Biological and Biomedical Applications. *Adv. Mater.* **2009**, *21*, 4880−4910.

(17) Park, H. S.; Agarwal, A.; Kotov, N. A.; Lavrentovich, O. D. Controllable Side-by-Side and End-to-End Assembly of Au Nanorods by Lyotropic Chromonic Materials. *Langmuir* **2008**, *24*, 13833−13837.
(18) Hasobe, T.; Imahori, H.; Kamat, P. V.; Ahn, T. K.; Kim, S. K.; Kim, D.; Fujimoto, A.; Hirakawa, T.; Fukuzumi, S. Photovoltaic Cells Using Composite Nanoclusters of Porphyrins and Fullerenes with Gold Nanoparticles. *J. Am. Chem. Soc.* **2005**, *127*, 1216−1228.
(19) (a) Poirier, G. E. Characterization of Organosulfur Molecular Monolayers on Au(111) Using Scanning Tunneling Microscopy. *Chem. Rev.* **1997**, *97*, 1117−1127. (b) Menendez, G.; Cortes, E.; Grumelli, D.; De Leo, L. P. M; Williams, F. J.; Tognalli, N. G.; Fainstein, A.; Vela, M. E.; Jares-Erijman, E. A.; Salvarezza, R. C. Self-Assembly of Thiolated Cyanine Aggregates on Au(111) and Au Nanoparticle Surfaces. *Nanoscale* **2012**, *4*, 531−540.
(20) Sun, D. Y.; Tham, F. S.; Reed, C. A.; Chaker, L.; Burgess, M.; Boyd, P. D. W. Porphyrin-Fullerene Host-Guest Chemistry. *J. Am. Chem. Soc.* **2000**, *122*, 10704−10705.